

AN XMM-NEWTON OBSERVATION OF NGC 1399 REVEALS TWO PHASES OF HOT GAS AND SUPER-SOLAR ABUNDANCES IN THE CENTRAL REGIONS

DAVID A. BUOTE

Department of Physics and Astronomy, University of California at Irvine, 4129 Frederick Reines Hall,
Irvine, CA 92697-4575; buote@uci.edu

Accepted for Publication in The Astrophysical Journal Letters

ABSTRACT

We present an initial analysis of a new *XMM* observation of NGC 1399, the central elliptical galaxy of the Fornax group. Spectral fitting of the spatially resolved spectral data of the EPIC MOS and pn CCDs reveals that a two-temperature model (2T) of the hot gas is favored over single-phase and cooling flow models within the central ~ 20 kpc. The preference for the 2T model applies whether or not the data are deprojected. The cooler component has a temperature (~ 0.9 keV) similar to the kinetic temperature of the stars while the hotter component has a temperature (~ 1.5 keV) characteristic of the virial temperature of a $\sim 10^{13} M_{\odot}$ halo. The two-phase model (and other multitemperature models) removes the “Fe Bias” within $r \lesssim 20$ kpc and gives $Z_{\text{Fe}}/Z_{\odot} \approx 1.5 - 2$. At larger radii the iron abundance decreases until $Z_{\text{Fe}}/Z_{\odot} \sim 0.5$ for $r \sim 50$ kpc. The Si abundance is super-solar (1.2-1.7 solar) within the central regions while $Z_{\text{Si}}/Z_{\text{Fe}} \approx 0.8$ over the entire region studied. These Fe and Si abundances imply that $\approx 80\%$ of the Fe mass within $r \sim 50$ kpc originates from Type Ia supernovae (SNIa). This SNIa fraction is similar to that inferred for the Sun and therefore suggests a stellar initial mass function similar to the Milky Way.

Subject headings: X-rays: galaxies: clusters – galaxies: halos – galaxies: formation – cooling flows

1. INTRODUCTION

NGC 1399, the central galaxy of the Fornax group, is one of the brightest elliptical galaxies in X-rays and has been the subject of numerous X-ray studies. Although previous *ROSAT* and *ASCA* studies demonstrated that the hot gas within $r \sim 30$ kpc is not isothermal (e.g., Rangarajan et al. 1995; Jones et al. 1997; Buote 1999), the data could not distinguish between single-phase and multiphase models. Moreover, we showed that an “Fe Bias” for systems like NGC 1399 occurs if an isothermal gas is assumed when in fact the spectrum consists of multiple temperature components with values near 1 keV (e.g., Buote 2000b,a). We argued that this bias is primarily responsible for the very sub-solar Fe abundances found in the central regions of the (X-ray) brightest ellipticals and groups.

The combined spatial and spectral resolution of the *XMM* CCDs allows for unprecedented mapping of the temperatures and elemental abundances of the hot gas in galaxies, groups, and clusters. These capabilities complement the high spatial resolution ($\sim 1''$) of *Chandra* which has already provided interesting constraints on the emission from discrete sources near the center of NGC 1399 (Angelini et al. 2001). The higher energy resolution, sensitivity, and larger field-of-view of the *XMM* EPIC CCDs are better suited for constraining the spatial and spectral properties of the diffuse hot gas out to radii well past the optical extent of the galaxy (i.e., out to $r \sim 50$ kpc assuming a distance of 21 Mpc using the results of Tonry et al. (2001) for $H_0 = 70 \text{ km s}^{-1} \text{ Mpc}^{-1}$).

We present initial results for the temperature and metal abundances of the hot gas obtained from a new *XMM* observation of NGC 1399. Detailed discussions of the data reduction, spectral fitting, and results for the gravitating mass will appear in Buote et al. (2002) and Lewis et al. (2002).

2. SPATIAL-SPECTRAL ANALYSIS

NGC 1399 was observed with the EPIC pn and MOS CCD cameras for approximately 25 ks and 30 ks respectively during AO-1 as part of the *XMM* Guest Observer program. We generated calibrated events lists for the data using the standard SAS v5.3.0 software. Our data preparation closely follows standard procedures and will be described fully in a follow-up paper (Buote et al. 2002).

We extracted spectra in concentric circular annuli located at the X-ray centroid of each detector. The widths of the annuli were the same for each detector and were defined such that the width of each annulus contained approximately 6000 background-subtracted counts in the 0.3-5 keV band in the MOS1, and the minimum width was set to $1'$ for PSF considerations. Obvious point sources were masked out before the extraction.

In each annulus we performed a simultaneous fit to the MOS1, MOS2, and pn spectral data over 0.3-5 keV. Our baseline model (1T) consists of a single thermal plasma component using the APEC code modified by foreground Galactic absorption ($N_{\text{H}} = 1.3 \times 10^{20} \text{ cm}^{-2}$) using the PHABS model in XSPEC v11.1.0v. The free parameters are all associated with the plasma component: temperature (T), normalization, and Fe, O, Mg, and Si abundances – all other elements tied to Fe in their solar ratios except for S which is tied to Si in their solar ratio. (The normalizations for the MOS1 and MOS2 are tied together while that of the pn is varied separately because of residual calibration and background differences.) We obtained results for the 1T model fitted directly to the data projected on the sky (i.e., 2D model) and also fitted to the deprojected data (i.e., 3D model) (e.g., Buote 2000a).

2.1. Two-Phase Temperature and Density Structure

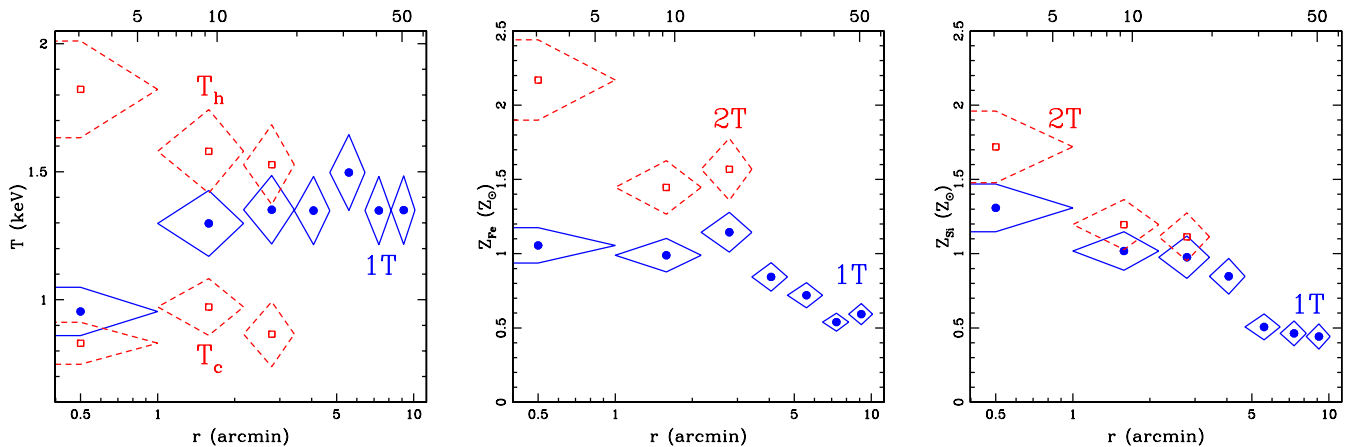


FIG. 1.— (Left panel) Radial temperature profiles (units – bottom: arcminutes, top: kpc) and 1σ errors for 1T and 2T models (both 2D). (Middle panel) The iron abundance profiles and (Right panel) the silicon abundance profiles of these models with 1σ errors.

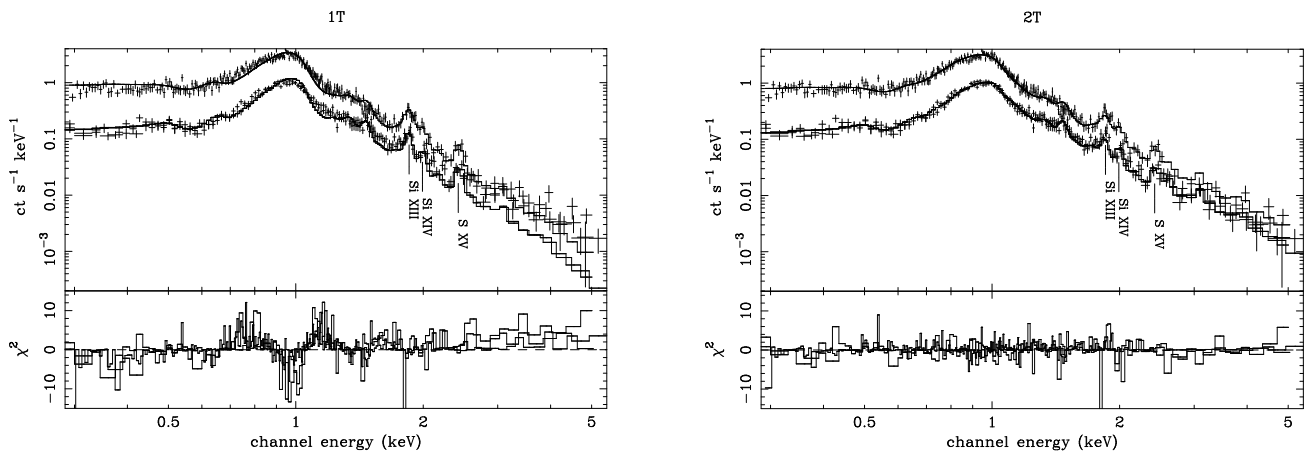


FIG. 2.— MOS and pn spectra for annulus #1 fitted with (Left panel) a 1T (2D) model and (Right panel) a 2T (2D) model.

TABLE 1
QUALITY OF SPECTRAL FITS

Annulus	R_{in} (arcmin)	R_{out} (arcmin)	1T		2T	
			χ^2	dof	χ^2	dof
1	0.0	1.0	1061.3	487	558.2	484
2	1.0	2.2	700.1	520	625.5	517
3	2.2	3.4	691.8	593	657.8	590
4	3.4	4.7	824.4	645		
5	4.7	6.5	925.3	776		
6	6.5	8.2	821.1	826		
7	8.2	10.1	1042.8	907		

The temperature profile for the 1T (2D) model is displayed in Figure 1. The temperature rises from $T \sim 0.9$ keV at the center to $T \sim 1.4$ keV at large radii consistent with previous 2D *ROSAT* determinations (e.g., Rangarajan et al. 1995; Jones et al. 1997; Buote 1999). This model is a good fit in the outer annuli but the fit degrades at progressively smaller radii (see Table 1). The worst fit is in the central annulus and, as shown in Figure 2, yields fit residuals near 1 keV that are fully characteristic of those obtained when trying to force a single-temperature model to fit a multi-temperature spectrum (e.g., Buote & Fabian 1998; Buote 1999, 2000b). The deviations above 2 keV also suggest the presence of another (higher) temperature component.

Multitemperature spectra in the inner regions, espe-

cially the central bin, can arise simply from the projection of hotter gas at larger radius. In this case fitting the 1T model to the deprojected spectra should substantially improve the fits in the central regions. However, we find that this 1T (3D) model does not improve the fits much except at the center, where noticeable – though relatively modest – improvement ($\Delta\chi^2 = 146$) is achieved.

We have examined a variety of multitemperature models (2D and 3D) and have found that simple two-temperature models (2T) provide the best fits to the central annuli (Table 1). It is also found that the χ^2 values are very similar and the derived parameters consistent within their 1σ errors for both 2D and 3D versions of the 2T models. And since the parameters of the 3D models are not as well constrained and require regularization of the temper-

atures and abundances (cf. Buote 2000a), in the interest of brevity we will emphasize in this letter the results for the 2D models. Detailed results for the 3D versions of 1T, 2T, and other models will appear in Buote et al. (2002).

With respect to the 1T (2D) model, not only does the 2T (2D) model improve the fit substantially within the central bin ($\Delta\chi^2 = 503$), but it also significantly improves the fits in annuli #2 ($\Delta\chi^2 = 75$) and #3 ($\Delta\chi^2 = 34$). The dramatic improvement in the central bin is seen in Figure 2 where the large residuals in the Fe L region near 1 keV have been mostly eliminated. In 3D the improvement of 2T over 1T is $\Delta\chi^2 = 363$ in the central bin. The other multitemperature models we examined only improved fits to the deprojected spectra in the central bins; e.g., a (constant pressure) cooling flow model consisting of ambient and cooling gas provides a modest improvement to the fit in the central bin ($\Delta\chi^2 = 99$) over the 1T (3D) model.

In Figure 1 are shown the temperatures obtained for the 2T (2D) model. The cool component is consistent with an isothermal radial profile while the hot component appears to rise slightly at the center. Within the 1σ errors this central rise for the hot component is not especially significant, but if real the slight excess over the isothermal extrapolation from the adjacent annuli probably represents the contribution from hard emission from discrete sources unresolved by *XMM* but resolved in the *Chandra* image of NGC 1399 (Angelini et al. 2001). We mention that adding an additional bremsstrahlung component to account for the effect of these unresolved sources (i.e., 2T+BREM) in the central bin does improve the fit slightly and gives a reasonable best-fitting temperature, $T \approx 5$ keV. Adding this component to the cooling flow model instead gives $T \approx 2.7$ keV indicating an attempt to account for both ~ 1 keV hot gas and ~ 5 keV unresolved sources.

We believe that in addition to the χ^2 values the derived parameter values also argue in favor of the 2T model. The temperature of the hot component, $T_h \sim 1.5$ keV, is consistent with the virial temperature of a surrounding group of mass $\approx 10^{13}M_\odot$, whereas the temperature of the cool component, $T_c \sim 0.9$ keV, is similar to the kinetic temperature of the stars ($T \sim 0.6$ keV) with velocity dispersion, $\sigma = 310$ km s $^{-1}$ (e.g., Jones et al. 1997). The volume-averaged electron density of the cool gas (n_e^c) declines with radius more rapidly than that of the hot component (n_e^h): for the best-fitting models the ratio n_e^c/n_e^h is 1.0, 0.62, and 0.27 respectively for shells #1, #2, and #3. (Here we have used the 3D model so that the quoted densities refer to the 3D spherical shells bounded by the same radii as the annuli listed in Table 1.) The cool component is only detected out to annulus #3 (i.e., for $r \lesssim 20$ kpc) and therefore must contribute even less at larger radius. The radius where the cool (galaxy) component gives way to the hot (group) component is similar to that inferred from the recent analysis of the *ROSAT* surface brightness profile of NGC 1399 by Paolillo et al. (2002).

Interior to shell #3 we compute a gravitating mass of $\approx 10^{12}M_\odot$ from each component consistent with previous X-ray (e.g., Rangarajan et al. 1995; Jones et al. 1997; Paolillo et al. 2002) and optical (e.g., Saglia et al. 2000) determinations. The consistency of the masses determined from each phase, and the agreement with optical determinations, indicates that each phase is in approximate hydro-

static equilibrium tracing the same gravitational potential.

Although hydrostatic equilibrium implies subsonic gas motions for each phase, the phases are not in pressure equilibrium. The ratio of the gas pressure in the hot phase to that of the cool phase is ≈ 2.4 in shell #1 which increases to ≈ 6.9 in shell #3. The lack of pressure equilibrium implies that the low-pressure cool phase must be continuously replenished. This requirement is consistent with the scenario where the cool phase continuously receives gas from stellar ejecta and loses gas by eventually mixing with the extended hot phase. Detailed physical models for the two phases (including, e.g., appropriate filling factors) will be considered in a future study.

2.2. Fe Abundance

We take the solar abundances in XSPEC to be those given by the Anders & Grevesse (1989) table except for Fe where we use the correct “meteoritic” value, Fe/H = 3.24×10^{-5} by number, as suggested by Ishimaru & Arimoto (1997) and McWilliam (1997). This value is 1.44 times smaller than the photospheric value which is usually employed in X-ray spectral fitting. Consequently, we shall account for this factor when comparing our results to other studies.

The Fe abundances (Z_{Fe}) obtained for the 1T and 2T models (both 2D) are displayed in Figure 1. (The values of Z_{Fe} obtained from 2D and 3D 2T models are consistent within 1-2 σ errors.) At the largest radii the abundance is sub-solar, $Z_{\text{Fe}}/Z_\odot \approx 0.5 - 0.6$. It increases for smaller r so that within $r \sim 20$ kpc, $Z_{\text{Fe}}/Z_\odot \approx 1$, for the 1T model similar to previous results for 1T (2D) models fitted to the *ROSAT* data (e.g., Jones et al. 1997; Buote 1999).

Compared to the 1T model, the 2T model gives Z_{Fe} that is 40%-50% larger in annuli #2 and #3 and twice as large in annulus #1. (A cooling flow model, when fitted to the deprojected spectra, produces similarly larger values.) This substantial increase in the value of Z_{Fe} along with the elimination of the characteristic ~ 1 keV residual pattern (Figure 2) is a manifestation of the “Fe Bias” we have discussed previously for NGC 1399 (Buote 1999) and related systems (e.g., Buote 2000b,a). We note that the abundances in each temperature component are tied together in the fits since they cannot be distinguished when fitted separately. Also, the values of Z_{Fe} deduced in the central bins for both 1T and 2T models differ slightly if intrinsic absorption is considered (which is not clearly required by the data as seen in Figure 2), but the relative differences between the 1T and 2T models and the general finding of super-solar values are preserved.

2.3. Si and S Abundances

Next to the broad feature of Fe L lines near 1 keV, the most notable spectral lines in the EPIC spectra of NGC 1399 (Figure 2) are the $K\alpha$ lines of Si and S; i.e., Si XIII He α (1.85 keV), Si XIV Ly α (2.0 keV), and S XV He α (2.45 keV). We find that Z_{Si} is generally better constrained than Z_{S} , but when these abundances are fitted separately they inevitably yield values that are consistent within their 1-2 σ errors. To reduce the number of free parameters in our fits we tie Z_{Si} and Z_{S} together in their solar ratio. Henceforth, we shall refer only to the Si abundance.

The Si abundance is plotted in Figure 1 for both 1T and 2T models. For the 1T model $Z_{\text{Si}}/Z_\odot \approx 0.5$ for $r \gtrsim 30$ kpc,

risers to values consistent with solar for $r \sim 5 - 20$ kpc, and is slightly larger than solar in the central bin. For the 1T model $Z_{\text{Si}}/Z_{\text{Fe}} \lesssim 1$ at large radii, $Z_{\text{Si}}/Z_{\text{Fe}} \sim 1$ for $r \sim 5 - 20$ kpc, and $Z_{\text{Si}}/Z_{\text{Fe}} \gtrsim 1$ in the central bin.

The 2T model gives slightly larger values, $Z_{\text{Si}}/Z_{\odot} \sim 1.1 - 1.2$ for $r \sim 5 - 20$ kpc (which are consistent with the 1T values within the 1σ errors). But in the central bin the 2T value is $\approx 30\%$ larger; i.e., about a 2σ discrepancy. In contrast to the 1T case, for the 2T model, $Z_{\text{Si}}/Z_{\text{Fe}} \approx 0.8$ for $r \lesssim 20$ kpc. (The overestimate of $Z_{\text{Si}}/Z_{\text{Fe}}$ using the 1T model is a ‘‘Si Bias’’ related to the Fe bias we discussed previously for such systems (Buote 2000b).)

(Unlike Fe and Si, the O and Mg abundances are quite sensitive to intrinsic absorption. We will discuss models with intrinsic absorption in Buote et al. (2002).)

3. CONCLUSIONS

We have performed a spatially resolved spectral analysis of the *XMM* EPIC data of NGC 1399 which suggests the presence of two dominant phases of hot gas within the central ~ 20 kpc. This two-phase description is consistent with 2T models we fitted previously to the *ASCA* data (Buote 1999). However, the *ASCA* data lacked the spatial resolution of *XMM* and could not distinguish between a radially varying single-phase medium, a two-phase medium, or a cooling flow within $r \sim 30$ kpc. These results for NGC 1399 are supported by previous analyses of its X-ray surface brightness profile which argues for separate galaxy and group components (e.g., Ikebe et al. 1996; Paolillo et al. 2002) similar to other centrally E-dominated groups (Mulchaey & Zabludoff 1998).

Since the temperature structure of NGC 1399 obtained by *ASCA* is characteristic of other central E-dominated galaxy groups (Buote 1999, 2000b; Buote et al. 1999; Allen et al. 2000), the two-phase structure revealed by *XMM* for NGC 1399 likely applies to these other systems. Moreover, since the centers of several clusters show similar multitemperature structure with *ASCA* (e.g., Buote et al. 1999; Allen et al. 2001) and similar multi-component surface brightness structure (see Ettori 2000, and references therein), we might expect two-phase structures in the centers of these systems. A recent *XMM* analysis of M87 is consistent with this suggestion (Molendi & Pizzolato 2001).

The two-phase model provides a physical explanation for the gas density and temperature profiles seen in ‘‘cooling flows’’. The hotter component is associated with the

ambient group or cluster gas while the cooler component is associated with the stellar ejecta of the dominant central galaxy. Gasdynamical models of groups and clusters constructed by Brighenti & Mathews (1999b, 2002b) demonstrate that relatively cool ejecta from stellar mass loss combined with the hotter ambient gas can reproduce observed single-phase temperature profiles in groups and clusters. But our results suggest that these two phases are not fully mixed.

Understanding the details of the interaction of these phases may shed light on the mystery of cooling flows. Using the results of Mathews (1989), the rate of energy input by stellar ejecta is, $\approx \alpha_* M_* \sigma^2$, where $\alpha_* \approx 5 \times 10^{-20} \text{ s}^{-1}$ is the specific stellar mass-loss rate. If within $r \sim 5$ kpc we take $M_* \approx 2 \times 10^{11} M_{\odot}$ for the stellar mass and $\sigma = 310 \text{ km s}^{-1}$ (Jones et al. 1997), we infer the rate of energy input into the central ~ 5 kpc of NGC 1399 from stellar ejecta to be $\approx 2 \times 10^{40} \text{ erg s}^{-1}$. This crude estimate is only a factor of two less than the X-ray luminosity of the hot component (and a factor of four less than the cool component). If the energy input from stellar ejecta does not completely suppress mass drop-out, it may at least delay the episodes of AGN feedback. Problems with such heating models are discussed by Brighenti & Mathews (2002a).

The two-phase model (as well as other multitemperature models) removes the ‘‘Fe Bias’’ within the central regions ($r \lesssim 20$ kpc) and gives $Z_{\text{Fe}}/Z_{\odot} \approx 1.5 - 2$. These supersolar values exceed the stellar values in typical elliptical galaxies (e.g., Trager et al. 2000) and therefore allow for significant enrichment of the hot gas from Type Ia supernovae (SNIa) (cf. Arimoto et al. 1997). For example, using the results of Gibson et al. (1997) and our measured value of $Z_{\text{Si}}/Z_{\text{Fe}} \approx 0.8$ solar, we infer that SNIa have contributed $\approx 80\%$ of the iron mass within $r \sim 50$ Kpc in NGC 1399. This SNIa fraction is similar to that inferred for the Sun and therefore suggests a stellar initial mass function similar to the Milky Way as advocated by Renzini and others (e.g., Renzini et al. 1993; Renzini 1997; Wyse 1997). We close by noting that although correcting for the ‘‘Fe Bias’’ partially removes the ‘‘Iron Discrepancy’’ noted by Arimoto et al. (1997), chemical models of elliptical galaxies without cooling flows predict central iron abundances even larger than we have measured for NGC 1399 (e.g., Brighenti & Mathews 1999a).

It is a pleasure to thank F. Brighenti, W. Mathews, and the anonymous referee for comments on the manuscript.

REFERENCES

- Allen, S. W., Di Matteo, T., & Fabian, A. C. 2000, *MNRAS*, 311, 493
- Allen, S. W., Fabian, A. C., Johnstone, R. M., Arnaud, K. A., & Nulsen, P. E. J. 2001, *MNRAS*, 322, 589
- Anders, E. & Grevesse, N. 1989, *Geochim. Cosmochim. Acta*, 53, 197
- Angelini, L., Loewenstein, M., & Mushotzky, R. F. 2001, *ApJ*, 557, L35
- Arimoto, N., Matsushita, K., Ishimaru, Y., Ohashi, T., & Renzini, A. 1997, *ApJ*, 477, 128
- Brighenti, F. & Mathews, W. G. 1999a, *ApJ*, 515, 542
- . 1999b, *ApJ*, 512, 65
- . 2002a, *ApJ*, in press (astro-ph/0203409)
- . 2002b, *ApJ*, 567, 130
- Buote, D. A. 1999, *MNRAS*, 309, 685
- . 2000a, *ApJ*, 539, 172
- . 2000b, *MNRAS*, 311, 176
- Buote, D. A., Canizares, C. R., & Fabian, A. C. 1999, *MNRAS*, 310, 483
- Buote, D. A. & Fabian, A. C. 1998, *MNRAS*, 296, 977
- Buote, D. A., Lewis, A. D., Brighenti, F., & Mathews, W. G. 2002, in preparation
- Ettori, S. 2000, *MNRAS*, 318, 1041
- Gibson, B. K., Loewenstein, M., & Mushotzky, R. F. 1997, *MNRAS*, 290, 623
- Ikebe, Y., Ezawa, H., Fukazawa, Y., Hirayama, M., Izhisaki, Y., Kikuchi, K., Kubo, H., Makishima, K., Matsushita, K., Ohashi, T., Takahashi, T., & Tamura, T. 1996, *Nature*, 379, 427
- Ishimaru, Y. & Arimoto, N. 1997, *PASJ*, 49, 1
- Jones, C., Stern, C., Forman, W., Breen, J., David, L., Tucker, W., & Franx, M. 1997, *ApJ*, 482, 143
- Lewis, A. D., Buote, D. A., Brighenti, F., & Mathews, W. G. 2002, in preparation
- Mathews, W. G. 1989, *AJ*, 97, 42

- McWilliam, A. 1997, *ARA&A*, 35, 503
Molendi, S. & Pizzolato, F. 2001, *ApJ*, 560, 194
Mulchaey, J. S. & Zabludoff, A. I. 1998, *ApJ*, 496, 73
Paolillo, M., Fabbiano, G., Peres, G., & Kim, D.-W. 2002, *ApJ*, 565, 883
Rangarajan, F. V. N., Fabian, A. C., Forman, W. R., & Jones, C. 1995, *MNRAS*, 272, 665
Renzini, A. 1997, *ApJ*, 488, 35
Renzini, A., Ciotti, L., D'Ercole, A., & Pellegrini, S. 1993, *ApJ*, 419, 52
Saglia, R. P., Kronawitter, A., Gerhard, O., & Bender, R. 2000, *AJ*, 119, 153
Tonry, J. L., Dressler, A., Blakeslee, J. P., Ajhar, E. A., Fletcher, A., Luppino, G. A., Metzger, M. R., & Moore, C. B. 2001, *ApJ*, 546, 681
Trager, S. C., Faber, S. M., Worthey, G., & González, J. J. . 2000, *AJ*, 119, 1645
Wyse, R. F. G. 1997, *ApJ*, 490, L69